A mean-field model of gamma-frequency oscillations in networks of excitatory and inhibitory neurons

Farzin Tahvili*and Alain Destexhe

Institute of Neuroscience (NeuroPSI),
Paris-Saclay University, CNRS, 91400 Saclay, France.

November 20, 2023

Abstract

Gamma oscillations are widely seen in the cerebral cortex in different states of the wake-sleep cycle and are thought to play a role in sensory processing and cognition. Here, we study the emergence of gamma oscillations at two levels, in networks of spiking neurons, and in a mean-field model. At the network level, we consider two different mechanisms to generate gamma oscillations and show that they are best seen if one takes into account the synaptic delay between neurons. At the mean-field level, we show that introducing a delay in the mean-field also produces gamma oscillations. The mean-field matches the mean activity of excitatory and inhibitory populations, as well as the oscillation frequency, for both mechanisms. This mean-field model of gamma oscillations should be a useful tool to investigate large-scale interactions through gamma oscillations in the brain.

Introduction

Information processing in the brain is based on dynamic interplay among different groups of neurons exhibiting various rhythmic patterns. These rhythmic activities of neurons vary significantly depending on different states of behavior and they are closely linked to specific sensory, motor, and cognitive functions. Low-frequency band ($< 10\ Hz$) oscillations could serve as temporal references (Kayser et al. 2012), whereas faster oscillations in beta and gamma frequency bands can be important for visual attention (Engel et al. 2001), feature selection (Gray et al. 1989) or binding (Engel et al. 2001). These oscillatory activities

*Present address: Stem-cell & Brain Research Institute (SBRI), 69500 Bron Cedex France

are observed throughout different brain structures across various species and therefore they can be considered as one of the main fingerprints of a typical nervous system.

Among different oscillation bands, the gamma band which is commonly observed during both waking and sleep states, has great importance especially because of its tight relationship to cognitive processes. Generally, oscillations with a frequency higher than 30 Hz are categorized in the gamma band (Buzsáki and Wang 2012). The gamma band can also be divided into sub-bands based on different strategies. As an example, in the hippocampal CA1 region, wavelet analysis identified three distinct gamma bands: slow gamma (30–50 Hz), mid-frequency gamma (50–90 Hz), and fast gamma (or epsilon band, 90–140 Hz) (Tort et al. 2010; Belluscio et al. 2012).

While the collective activity (like the LFP signal) exhibits synchronized oscillations, the individual firing patterns of neurons tend to be irregular and infrequent. This activity regime which is the typical observing state in the cortex in vivo, is known as the Asynchronous Irregular (AI) state and has the following characteristics (Brunel 2000). This kind of activity places cortical neurons close to their firing threshold rather than resting potential and therefore the response of the system to a stimulus will be much faster than the one at rest. In this regime, neurons are subjected to the bombardment from many inputs so it implies that the excitatory and inhibitory inputs should balance each other and neurons kept around their firing threshold so they fire based on noise fluctuations.

When neurons receive stochastic inputs and fire spikes irregularly, sufficiently strong recurrent synaptic interactions will make the asynchronous state unstable against random fluctuations, and oscillations emerge (Brunel 2000, Brunel and Wang 2003, Geisler et al. 2005). In particular, it has been demonstrated that often these oscillations emerge from asynchronous states via Hopf bifurcations in the presence of an additional time scale, beyond the one associated with the neuron membrane potential evolution, which can be the transmission delay or a finite synaptic timescale. As the frequency of these oscillations is related to such external timescales, this mechanism is normally related to fast oscillations (Di Volo and Torcini 2018).

The important properties of experimentally observed gamma oscillations are as follows (Buzsáki and Wang 2012). Firstly, Gamma oscillations are short-lived and emerge from the coordinated interactions of excitation and inhibition. Secondly, different sub-bands of gamma oscillations can coexist or occur in isolation. Thirdly, gamma-band rhythmogenesis is inextricably tied to inhibition. Fourthly, gamma rhythm typically concurs with irregular firing of single neurons, and the network frequency of gamma oscillations varies extensively depending on the underlying mechanism. Fifthly, the magnitude of gamma oscillation is modulated by slower rhythms.

Gamma oscillations have been described in several areas of the neocortex (Sirota et al. 2008), entorhinal cortex (Chrobak and Buzsaki 1998), amygdala (Popescu et al. 2009), hippocampus (Mann et al. 2005), striatum (Berke et al 2004), and thalamus (Pinault and Deschênes 1992) as well as other areas. Common properties of these brain regions are the presence of inhibitory interneurons and their actions through GABA A receptors. The consistent patterns of gamma frequency oscillations across various brain regions and species offer insights into the necessary mechanisms that support them.

Minimally, only three requirements are needed for gamma oscillations to emerge (Wang and Buzsáki 1996): mutually connected inhibitory interneurons, a time constant provided by GABA A receptors, and sufficient drive to induce spiking in the interneurons. The emerging synchrony is caused when a subset of the interneurons begins to discharge together and generates synchronous IPSPs in the partner neurons. In turn, the inhibited neurons will spike again with increased probability when GABA A receptor-mediated hyperpolarization has decayed, and the cycle repeats. The frequency of gamma oscillation in the I-I model is determined mainly by the kinetics of the IPSPs and the net excitation of interneurons.

In this study, we work with conductance-based sparse spiking networks that consist of two types of neurons, pyramidal regular spiking neurons and parvalbumin fast-spiking interneurons (RS-FS networks), and investigate the genesis of gamma rhythms in them. We offer the corresponding mean-field model in parallel and illustrate that it is in perfect agreement with the spiking networks. Throughout this study, we investigate the role of synaptic delay with specific attention due to its proved important role (Brunel and Wang 2003).

The objective of the present work is to investigate the gamma oscillation emergence during the AI state and provide the mean-field model which is in very good agreement with spiking networks. We investigate two mechanisms that result in gamma oscillations appearing, synaptic delay and excitation-inhibition balance break. We explore spiking network models and their corresponding mean-field and discuss in which experimental conditions they can be realistic. Furthermore, we discuss that some experimentally observed characteristics of gamma oscillations that were mentioned before can be observed in our models well and so this shows that our models may be close to reality.

Materials and Methods

Neuron and Network

As our neuronal units, we use the AdEx model. In this model, each neuron i is described by its membrane potential V_i, which evolves according to the following

equations:

$$
\begin{aligned}
C\frac{dV_i(t)}{dt} &= -g_L\left(V_i - E_L\right) + g_L\Delta\exp\left[\frac{(V_i(t)-V_{th})}{\Delta}\right] - w_i(t) - I_{syn_i}(t)\\
I_{syn_i}(t) &= g_{E_i}(t)\left(V_i(t)-E_E\right) + g_{I_i}(t)\left(V_i(t)-E_I\right)\\
\tau_{E,I}\frac{dg_{E,I_i}(t)}{dt} &= -g_{E,I_i}(t) + Q_{E,I_i}\sum_k \delta\left(t-t_k\right)\\
\tau_w\frac{dw_i(t)}{dt} &= a\left(V_i(t)-E_L\right) - w_i(t) + b\sum_j \delta\left(t-t_j\right)
\end{aligned}
$$

Where C is the neuron membrane capacitance, g_L is the leakage conductance, E_L is the leaky membrane potential, V_{th} is the effective threshold and Δ is the threshold slope factor. The synaptic current, I_{syn_i}(t), received from other neurons to neuron i is taken into account as conductance-based. Every time a presynaptic neuron spikes at time t_k, the excitatory g_{E_i} or the inhibitory g_{I_i} synaptic conductance increases by a discrete amount Q_E or Q_I (excitatory or inhibitory synaptic strength), depending on the nature of the presynaptic neuron. Synaptic conductances subsequently decay exponentially with a time constant τ_E or τ_I. E_E and E_I are the reversal potential of excitatory and inhibitory synapses, respectively. The Σ_k runs over all the presynaptic excitatory or inhibitory neurons spike times. During the simulations, the equation characterizing the membrane potential V_i is integrated until a spike is generated. In practice, the spiking time is defined as the moment in which V_i reaches a certain threshold (V_{cut}). Then the membrane potential is reset to V_{rest}, which is kept constant until the end of the refractory period T_{ref}. After the refractory period, the equations start being integrated again. The adaptation current is described by the variable w_i. It increases by an amount b every time that neuron i emits a spike at times t_j and decays exponentially with time scale τ_w. The parameter a indicates the sub-threshold adaptation. For the specific values of the parameters, one can see Table 1 and Table 2.

We consider two types of synapses between our neurons, excitatory and inhibitory synapses. For determining the time scale of the excitatory synapse, we consider that such a synapse is composed of 10% NMDA receptors and the rest (90%) AMPA receptors and this leads to a net time scale equals 5 ms (Destexhe). For the inhibitory synapses which we suppose that they only include GABA A receptors, the time scale is considered equal to 5 ms (Brunel and Wang 2003). One can see Table 2 which shows synaptic parameters including synaptic conductance quantals Q_E and Q_I, synaptic time scales τ_E and τ_I, and synaptic delay τ_d.

Our networks are composed of $N = 10000$ neurons, 80% Regular spiking, and 20% of Fast spiking cells. All neurons are connected randomly with the probability p which we consider equal to 0.05 . In addition to recurrent connections, each neuron receives an external drive. The drive is implemented as 8000 in-

dependent and identically distributed Poissonian spike trains with the spiking frequency μ (The typical value of μ in our simulations is 3 Hz), being sent to the network with the probability of connection p. These spike trains are computed inside of the synaptic current term through a discontinuous increase of the excitatory synaptic conductance g_E by the amount Q_E.

Table 1. Neuron parameters.

Parameter	Regular spiking cell	Fast spiking cell
V_{th}	-50 mV	-50 mV
V_{cut}	-40 mV	-47.5 mV
Δ	2 mV	0.5 mV
T_{ref}	5 ms	5 ms
τ_w	500 ms	500 ms
a	4 nS	0 nS
b	60 pA	0 pA
C	200 pF	200 pF
g_L	10 nS	10 nS
E_L	-65 mV	-65 mV
V_{rest}	-65 mV	-65 mV

Table 2. Synapse parameters

Parameter	Value
τ_E	5 ms
τ_I	5 ms
E_E	0 mV
E_I	-80 mV
Q_E	1.3 nS
Q_I	5 nS
τ_d	$Variable$

Throughout the study, we determine the population activity of the spiking network as follows: We employ the population activity definition,

$$v(t) = \lim_{\Delta t \to 0} \frac{1}{\Delta t} \frac{n_{\text{act}}(t, t + \Delta t)}{N}$$

which allows us to calculate the population activity for both the RS and FS populations after simulating the spiking network. In this formula, N represents the number of neurons within the specific population, such as FS and RS populations. The term $n_{act}(t, t + \Delta t)$ signifies the cumulative spike count across all neurons in the group within the time window $(t, t + \Delta t)$. Throughout our study, we consistently set Δt to 0.1 ms for calculating spiking network population activities. After calculating the population activities, we perform Fourier analysis

on them and plot the spectrum of the signals. We choose the frequency which has the maximum power as the frequency of oscillation.

Mean-Field

The mean-field model consists of a model introduced previously (Di Volo et al. 2019), which consists of two populations of RS and FS neurons with adaptation. This model was based on a Master Equation formalism to derive mean-fields of spiking neurons (El Boustani and Destexhe, 2009), and which was extended to model networks of RS and FS cells described by the AdEx model. The version of Di Volo et al. (2019) included adaptation and closely matched the spontaneous activity as well as the response of the network to external inputs. The main modification to this model is that we introduced time delays to match the synaptic delay in the spiking network. Our mean-field dynamics are as follows:

$$\begin{aligned} T\partial_t v_E &= F_E\left(v_E\left(\mathrm{t}-r\tau_d\right), v_I\left(\mathrm{t}-\tau_d\right), w\right) - v_E \\ T\partial_t v_I &= F_I\left(v_E\left(\mathrm{t}-\tau_d\right), v_I\left(\mathrm{t}-\tau_d\right)\right) - v_I \\ \partial_t w &= -\frac{w}{\tau_w} + b v_E + a\left(\mu_V\left(v_E\left(\mathrm{t}-\tau_d\right), v_I\left(\mathrm{t}-\tau_d\right), w\right) - E_L\right) \end{aligned}$$

v_E and v_I are the mean population activities of RS and FS populations, respectively. F_E and F_I are RS and FS transfer functions. τ_d is the time delay that mimics the role of synaptic delay in the spiking network and r is a constant equal to 1.3 . w is the adaptation factor and a and b are adaptation parameters same as in the spiking network. μ_V is the RS average population voltage which is a function of v_E, v_I, and w (for further information about the calculation of μ_V, one can see Zerlaut et al. 2018). E_L is the leak voltage which equals that of the spiking network. The equation for the FS population has no term w since the adaptation of FS neurons is considered to be zero. T is the time scale of the mean-field dynamics. On the principles of the mean-field theory, T must be in the range in which the system acts as a Markovian system. However, if we put it high, the mean-field cannot capture gamma oscillations. Throughout the study, we consider T = 5 ms and so we ensure that we can capture all the frequencies below $\frac{1}{T}$ which is 200 Hz.

We use the Ornstein-Uhlenbeck process as the noise in our mean-field model which is the only nontrivial process that satisfies Gaussian, Markovian, and temporally homogeneous properties. The noise is defined by the following equation $dX(t) = -X(t)\theta dt + \sigma dW(t)$, where σ and θ are parameters and $W(t)$ is the standard Brownian motion. We take the timescale of the noise equal to 5 ms which results in choosing $\theta = 200\ Hz$. This amount of timescale is the same as in Di Volo et al. 2019, where they model Up and Down states. By doing this, on the one hand, we ensure that all frequencies below 200 Hz exist in the noise with comparable power, and on the other hand, it is completely compatible with the configuration of the mean-field which explains Up-Down states.

Simulation

Spiking networks are simulated under the Brian 2 Python package and their corresponding mean-fields are simulated under Python. All equations are numerically integrated using Euler's Method with $dt = 0.1ms$ as the integration time step (smaller time steps also lead to similar results).

Results

In this section, we investigate two types of networks where gamma oscillations can appear, which we call Type 1 and Type 2. From the perspective of parameters, the only difference between them is that in Type 1 the power of the external drive on both populations is equal, while in Type 2 the power of the external drive on the RS population is higher than that of the FS population. We model them in the spiking network and show that the mean-field matches well with the spiking network in both cases.

Type 1 networks

In Type 1 networks, we consider the situation in which the external noise drive is the same for both populations. We illustrate that in this case, the synaptic delay plays a major role in the generation of gamma oscillations.

Figure 1 shows the dynamics of the spiking network without delay and its frequency analysis. One can see that only very fast oscillations can be seen from the raster, the membrane potential, or RS and FS population activities. This is also confirmed by the frequency analysis of the network activity. The corresponding mean-field is shown in Fig 2 and is in excellent agreement with the firing rates of the spiking network.

The situation is different when one considers a synaptic delay in the system. At the level of the spiking network, Fig. 3 clearly shows a prominent oscillation in which one can see the frequency of oscillation is around 100Hz in both populations.

These features are consistent with the mean-field model with delay. The corresponding mean-field for a delay of 2 ms is shown in Fig. 4, and one can see that it matches very well the spiking network in terms of both the frequency of oscillation and the mean activities. Also one can compare the power spectrum and Fourier transforms of the mean-field (Fig. 4) to those of the network (Fig. 3), and one can also see that the power of oscillation in the FS population is higher than that of RS, similar to the spiking network.

The same observations hold for a delay of 4 ms (Fig. 5 for the spiking network, and Fig. 6 for the mean-field). In this case, the oscillation is around 65Hz, and the mean-field matches well the oscillation frequency, and the activities of RS and FS cell populations. Moreover, one can see that when we increase the delay, the synchrony increases, and the magnitudes of oscillations become larger.

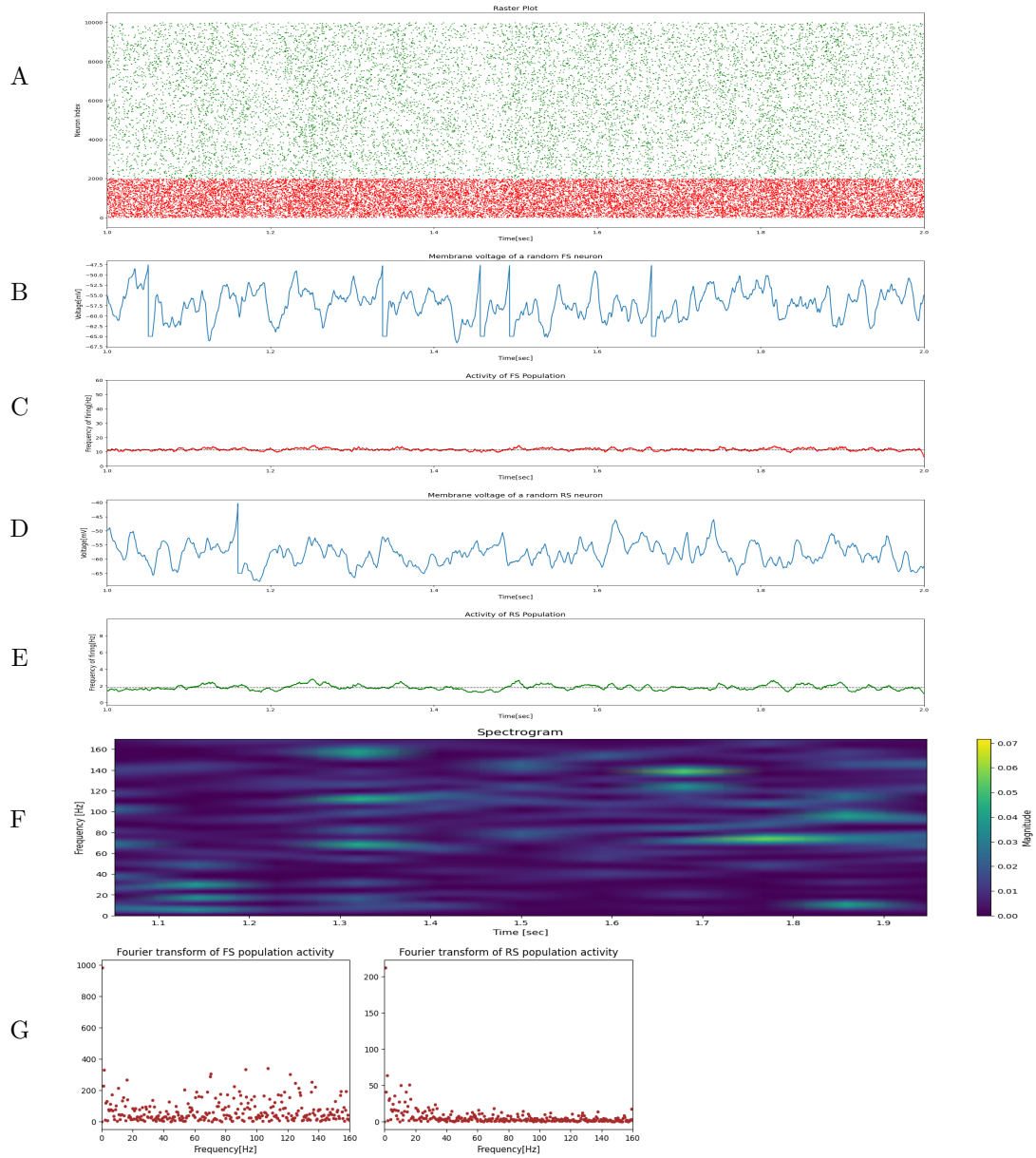

Figure 1: Type 1 spiking network with zero delay. The RS-FS spiking network is considered here with no delay. A. Raster of the spiking activity of RS (green) and FS (red) cells. B. Membrane potential of a random FS neuron (spikes are shown by vertical lines). C. Activity of the FS population. D. Membrane potential of a random RS cell (spikes are shown by vertical lines). E. Activity of the RS population. F. Spectrogram of FS population activity. G. Fourier transforms of FS and RS population activities on the whole time interval. No obvious dominant peak is visible.

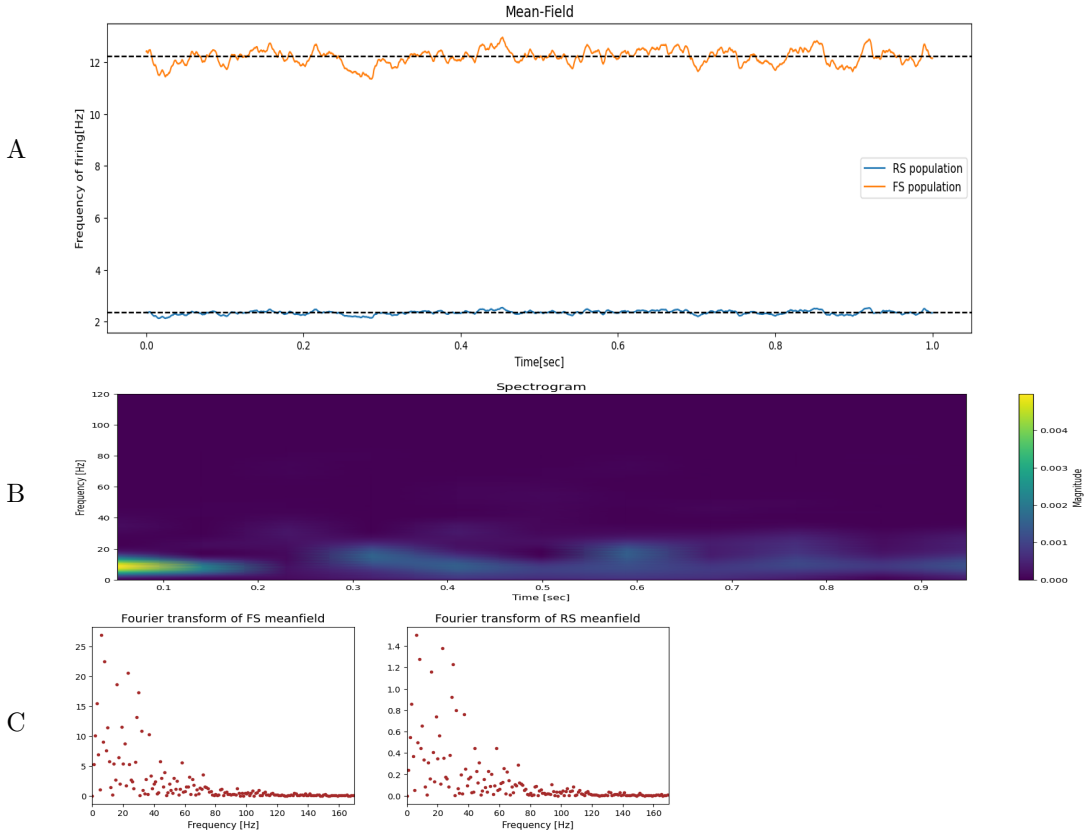

Figure 2: Simulated mean-field corresponding to the network in Fig. 1. A. Mean-field of the spiking network (Orange and blue are for FS and RS, respectively). B. Spectrogram of the FS mean activity. C. Fourier transforms of FS and RS mean activities on the whole time interval. No dominant oscillation peak is visible, in agreement with the corresponding spiking network in Fig. 1. FS and RS mean firing rates are very close to that of the spiking network.

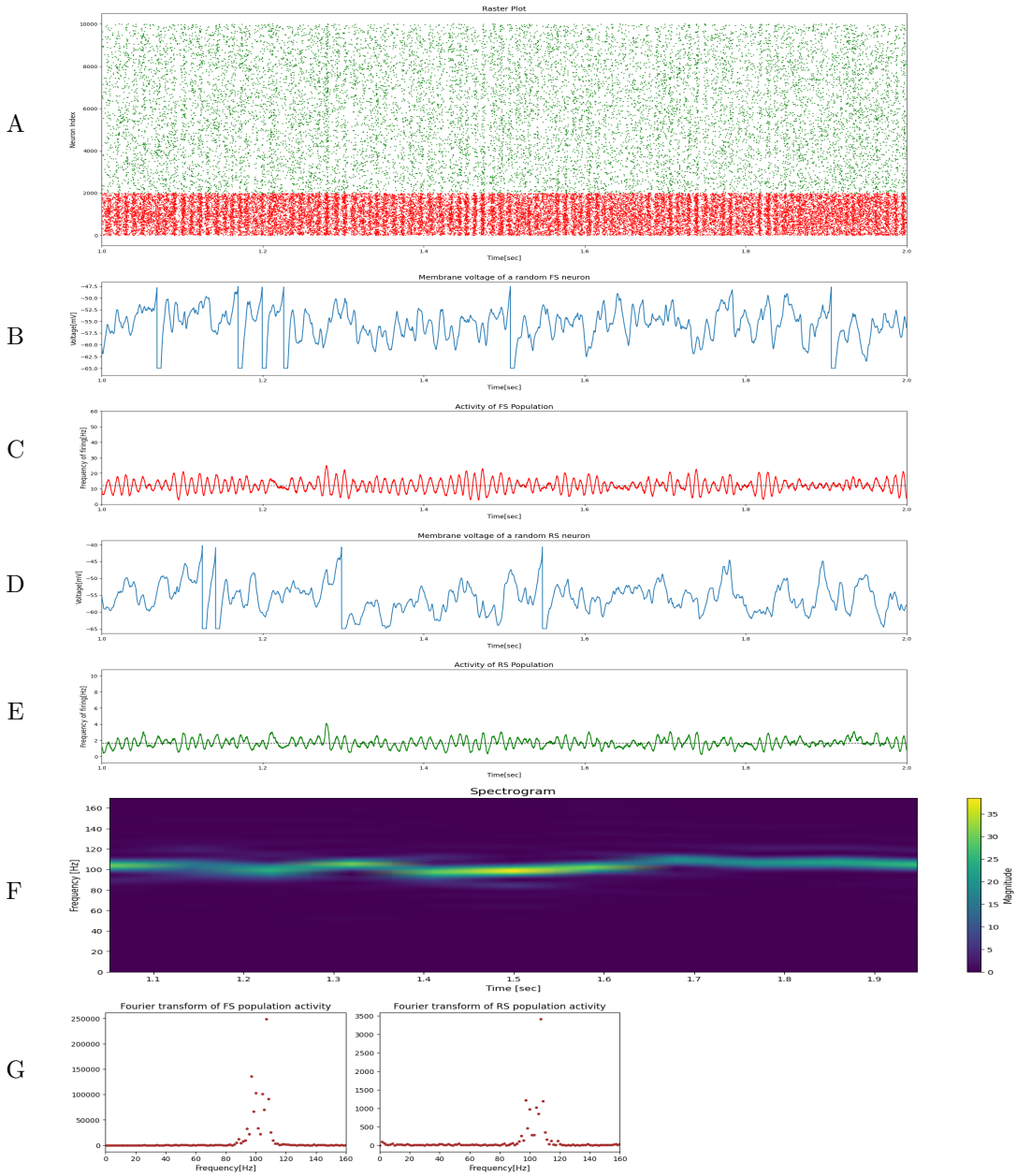

Figure 3: Activity of the type 1 spiking network with a synaptic delay of 2ms. Same arrangement of panels as for Fig. 1. The system has a prominent oscillation of around 100Hz as seen through the Spectrogram and Fourier transform curves. The power of oscillation in the FS population is higher than that of the RS population. Furthermore, the activities of RS and FS are in-phase.

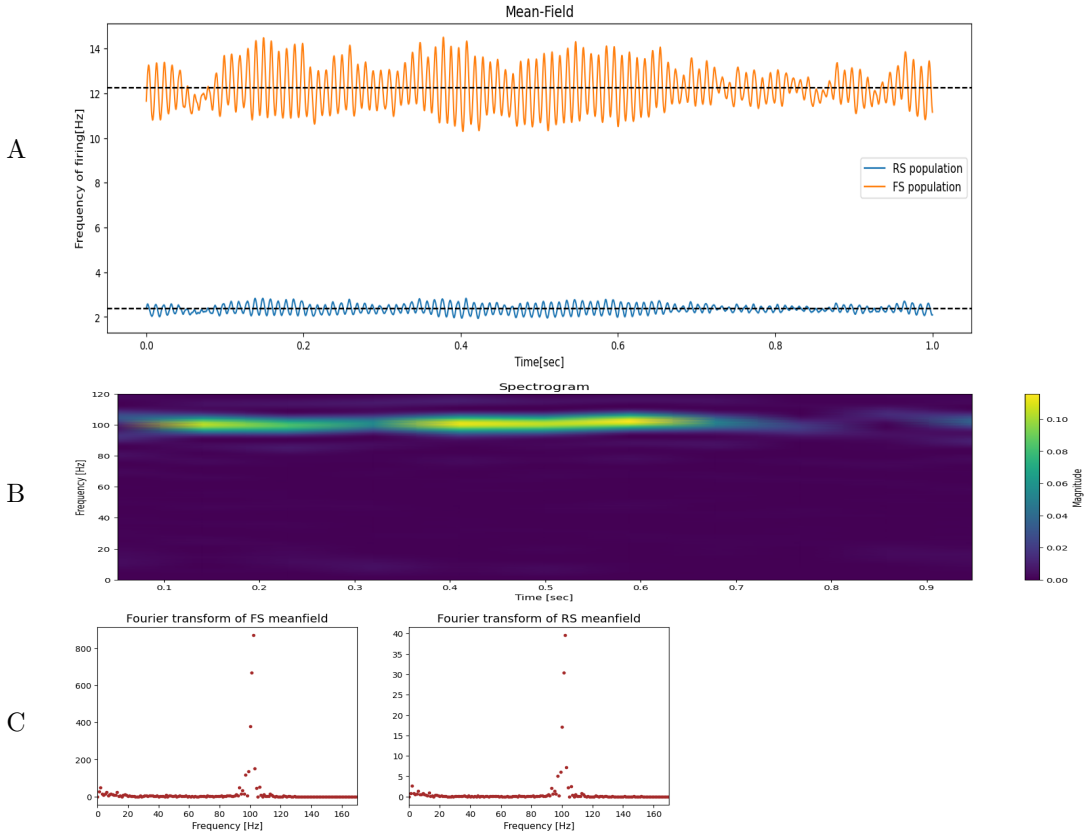

Figure 4: Simulated mean-field corresponding to the network of Fig. 3. Same arrangement of panels as for Fig. 2. The mean-field model is in very good agreement with the spiking network in terms of both population mean values and the oscillation. As one can see the frequency of oscillation is around 100Hz which is in very good agreement with the spiking network in Fig. 3. The power of oscillation in the FS population is higher than that of the RS population as in the spiking network. The FS and RS mean activities are in phase, similarly to the spiking network.

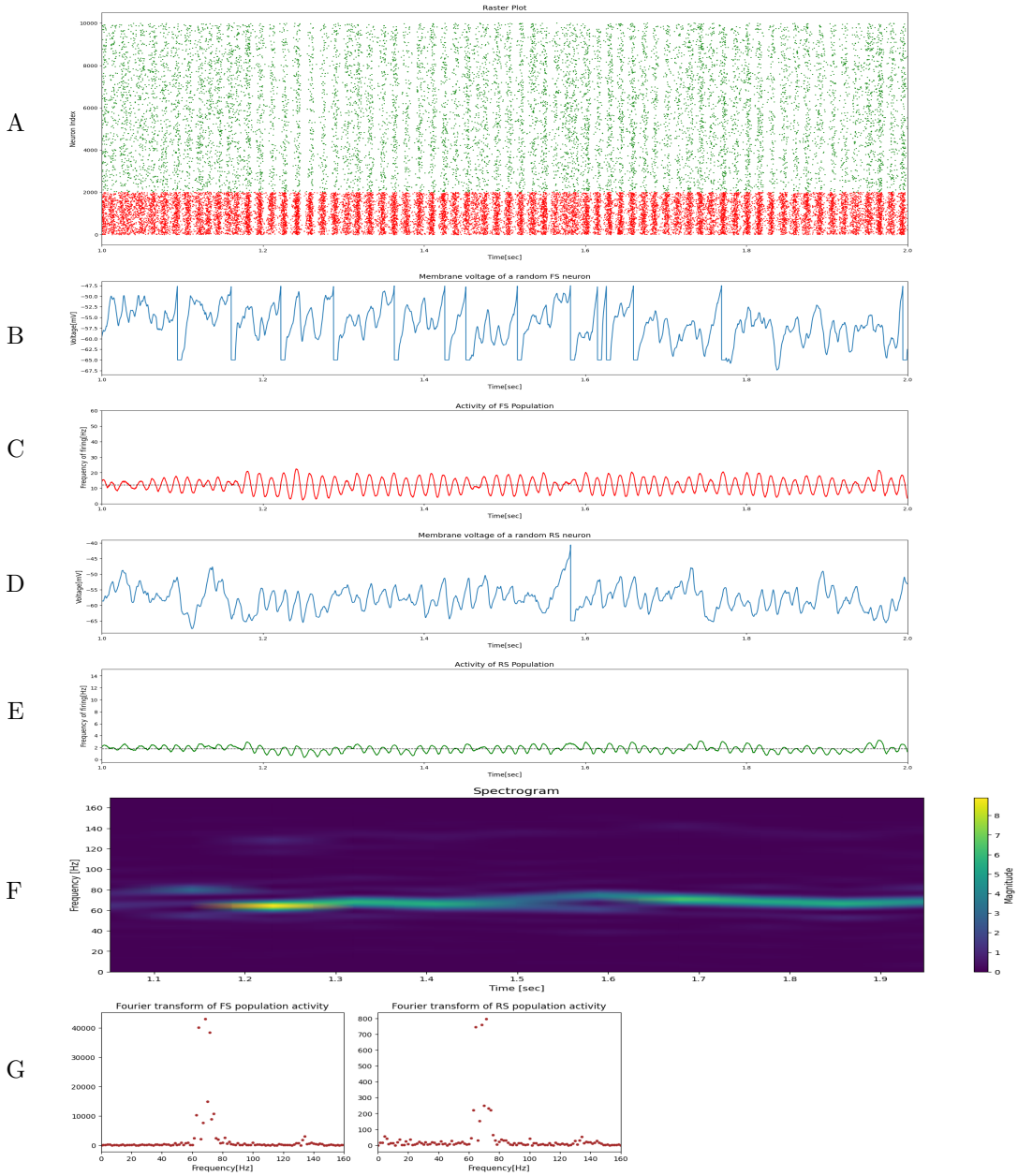

Figure 5: Activity of the type 1 spiking network with a synaptic delay of 4ms. Same arrangement of panels as for Fig. 1. There is a prominent oscillation of around 65Hz in the system as one can see through the Spectrogram and Fourier transform curves. The power of the oscillation in the FS population is much higher than that of the RS population. Furthermore, the activities of RS and FS are in-phase.

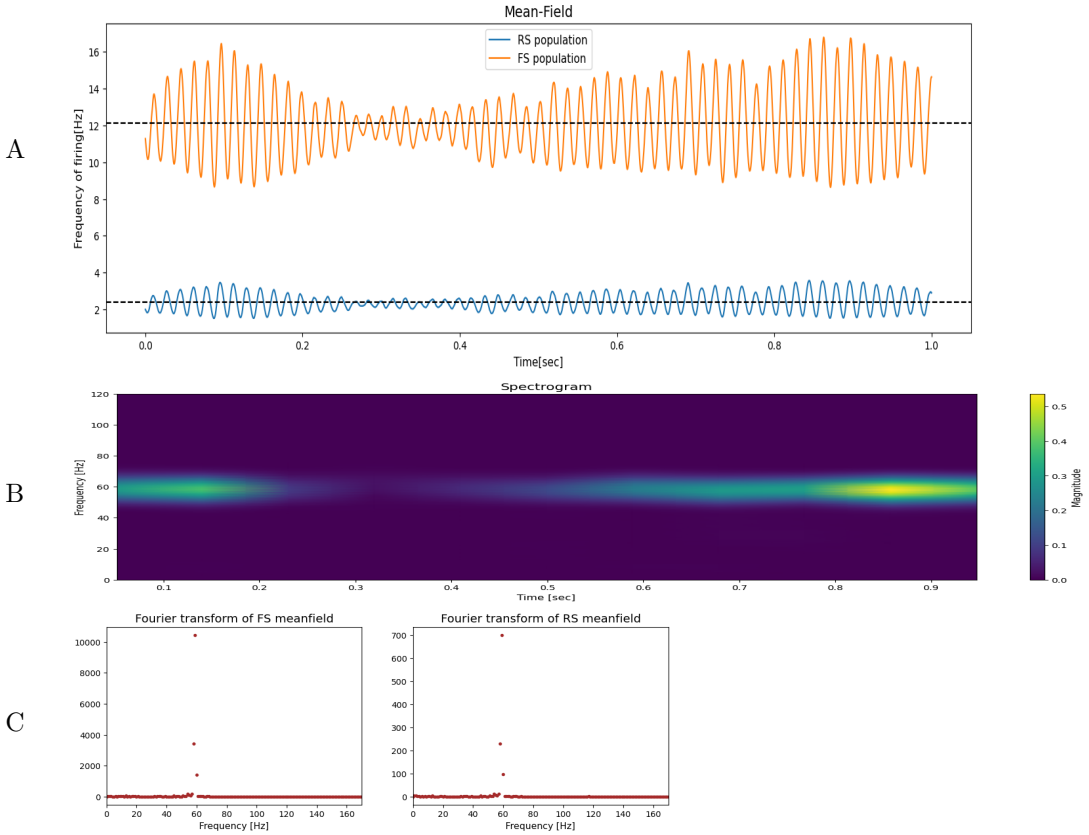

Figure 6: Simulated mean-field corresponding to the network Fig. 5. Same arrangement of panels as for Fig. 2. The mean-field model is in very good agreement with the spiking network in terms of both population mean values and the oscillation frequency. The frequency of oscillation is around 60Hz which is in agreement with the spiking network in Fig. 5. The power of oscillation in the FS population is much higher than that of the RS population as in the spiking network. Furthermore, the activities of RS and FS are in phase, similarly to the spiking network.

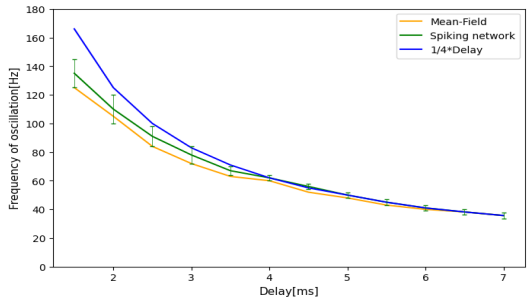

Figure 7: Frequency of oscillation as a function of synaptic delay in Type 1 networks. The mean-field frequency matches well with that of the spiking network. Moreover, they can be well fitted by $f = \frac{1}{4\tau_d}$, especially for larger delays.

So, for Type 1 networks, we conclude the following. First, as one increases the synaptic delay, the network synchrony and the ratio of gamma energy are amplified (One can see it by comparing the power of oscillations of Fig. 1, Fig. 3 and Fig. 5 shown besides Spectrograms). Secondly, Oscillations in RS and FS populations are in phase. This is the case for all spiking networks and their corresponding mean-field. Thirdly, the Power of gamma in the FS population is much higher than that of the RS population (one can see this through all Fourier transform figures). Figure 7 shows a synthesis of the network simulations and the corresponding mean-field. One can see that there is an excellent agreement between the spiking network and its mean-field in terms of the frequency of oscillation. Moreover, they can be well fitted by $f = \frac{1}{4\tau_d}$, especially for large delays as is obvious in the figure.

Type 2 networks

In this case, we consider the situation in which we can apply a lower drive on the FS population compared to that of the RS population. This case could correspond to drugs that would decrease the synaptic input to FS cells, or to brain areas where the external input is weaker on FS cells. In such cases, we artificially break the excitation-inhibition balance. As noted in the introduction, breaking the excitation-inhibition balance is one of the mechanisms for gamma oscillation emergence.

Indeed, when simulating Type 2 RS-FS spiking networks, we observe the genesis of gamma oscillations, as shown in Fig. 8 for a delay of 3 ms where one can see that the frequency of oscillation is around 60Hz. In this case, the power of the oscillation is comparable for RS and FS cells, and the oscillation peaks are rather broad.

Similar to Type 1 networks, there is a good match between the spiking network and the mean-field in terms of both frequency of oscillation and mean

activity values, as one can see by comparing Figs. 8 and 9. Similar to the spiking network, the mean-field produced an oscillation around 60 Hz, and the firing levels of RS and FS cells are comparable, compared to Type 1 networks. Thus, there is a good general agreement between the mean-field and the spiking network for Type 2 as well. This relation is further shown in Fig. 10, where one can see that the gamma oscillation frequency predicted by the mean-field closely matches the frequency of the Type 2 spiking network.

Discussion

In this study, we have explored spiking networks and respective mean-field models for the generation of gamma oscillations during the AI state in the Cortex and illustrated that they match well with each other. We have studied two types of configurations. In Type 1 networks, the oscillation is generated by the interplay of excitation and inhibition (RS and FS cells in our model), and the synaptic time delay is essential in this mechanism. We have shown that the network oscillation is a decreasing function of the time delay (Fig. 7), which can be well fitted by $f = \frac{1}{4\tau_d}$. It must be noted that here, the synaptic time delay accounts for the axonal and synaptic delays, which may be constant in a local network because the axonal connections are short-range. In the case of large-distance connections, the axonal delay will be proportional to distance, and one could expect more complex behavior in such multiple-time delay systems.

We also showed that for Type 1 networks, the mean-field model, if equipped with time delays, can produce gamma oscillations. The agreement between the oscillation frequency predicted by the mean-field and the spiking network is remarkable (Fig. 7). It must be noted that this agreement is not in contradiction with the Markovian hypothesis which is central in the formalism (El Boustani and Destexhe, 2009). The condition is that the time constant T of the mean-field must be smaller, or at maximum comparable to, the oscillation period of gamma oscillations. This may be challenging for the small values of delay, where the oscillation frequency is high (Fig. 7), but astonishingly the mean-field still predicts well the oscillation frequency.

A second type of mechanism was considered for the genesis of gamma oscillations, based on a break-down of the balance between excitation and inhibition. In these Type 2 networks, the external drive was reduced on FS cells. As a result, FS cells exerted less inhibitory overall activity and the mean firing rate of RS cells augmented (around 4 Hz in Type 2 networks, against around 2 Hz in Type 1; see Fig. 9 compared to Figs. 2 and 4). This produces a different type of gamma oscillation with a lower oscillation frequency (compare Fig. 7 and Fig. 10). Here again, there was a remarkable match between the network frequency and the frequency predicted by the mean-field (Fig. 10). In this case, however, the mean-field tended to produce more regular oscillations compared to the spiking network.

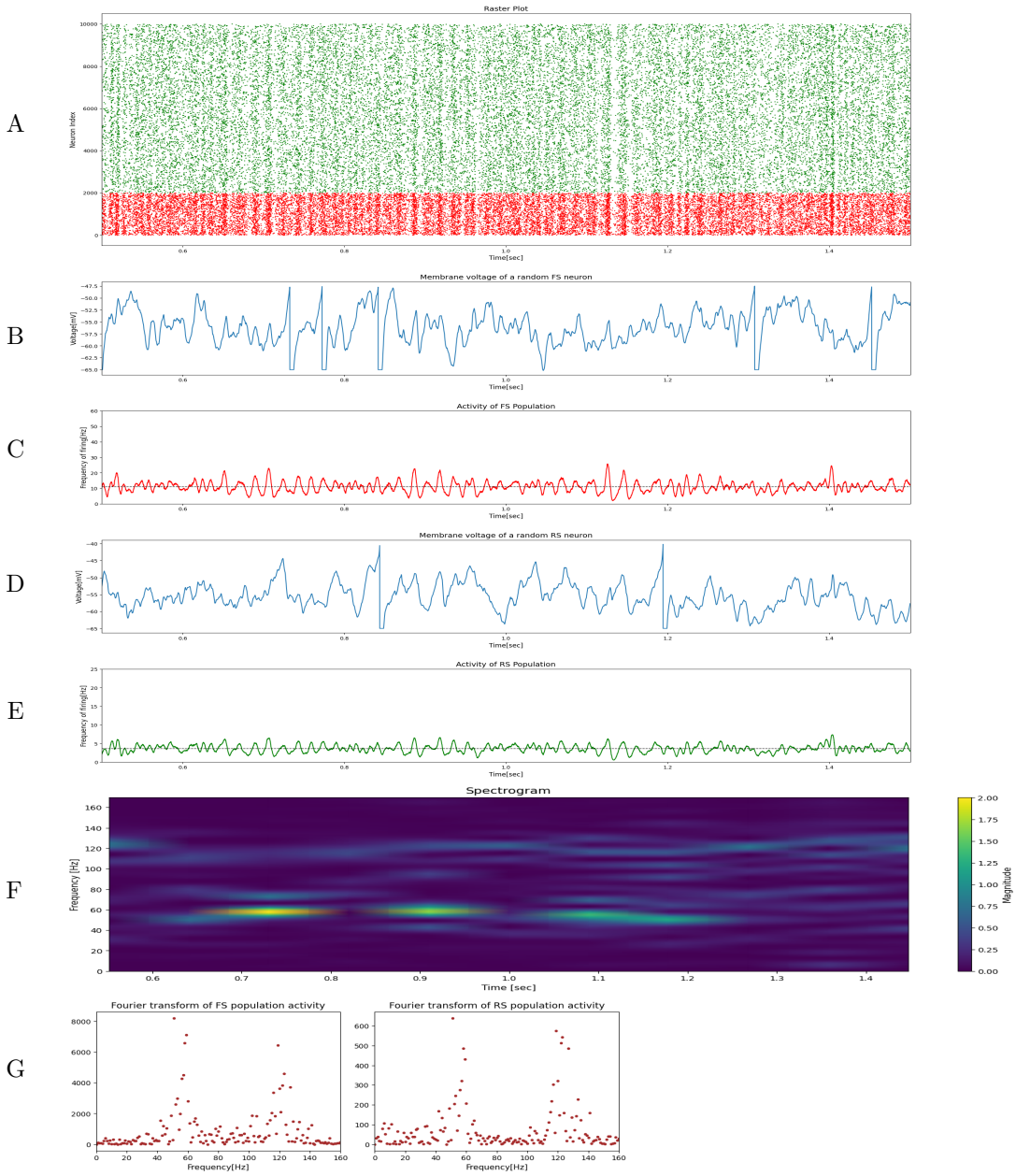

Figure 8: Activity of the type 2 spiking network with a synaptic delay of 3 ms. Same arrangement of panels as for Fig1. There is a prominent oscillation of around 50 Hz in the system as one can see through the Spectrogram and Fourier transform curves. The power of oscillation in the FS population is higher than that of the RS population.

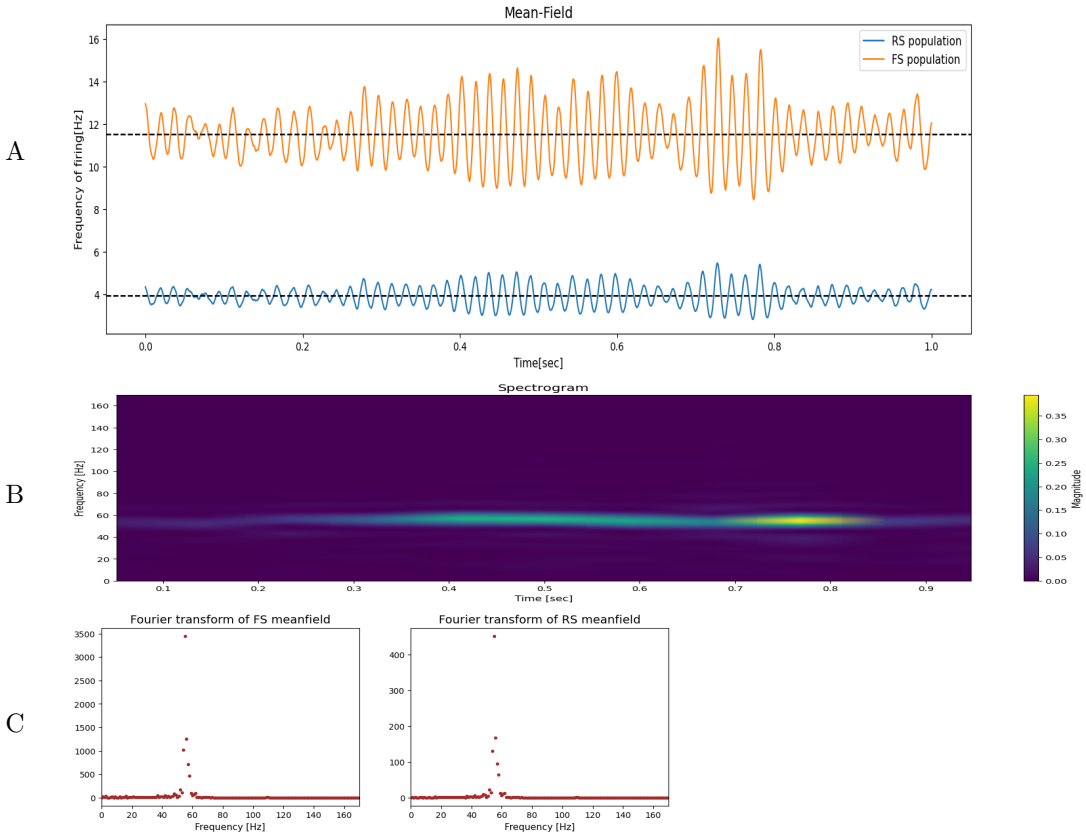

Figure 9: Simulated mean-field corresponding to the network Fig8. Same arrangement of panels as for Fig2. The mean-field model is in very good agreement with the spiking network in terms of both population mean values and the oscillation frequency. The frequency of oscillation is around 60 Hz which is in good agreement with the spiking network in Fig8. The power of oscillation in the FS population is higher than that of the RS population, as in the spiking network. Furthermore, the activities of RS and FS are in phase.

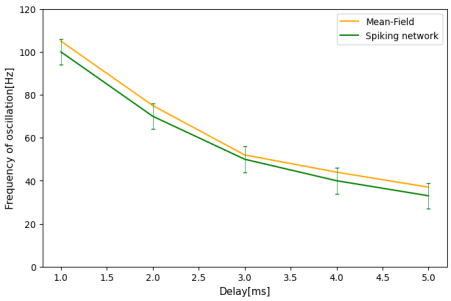

Figure 10: Relation between the frequency of oscillation and the delay for Type 2 networks. The ratio of drive on the RS population to that of the FS population is $\frac{3}{2}$.

Type 2 gamma oscillations also reveal another limitation of the mean-field formalism. In Fig. 8, one can clearly see two oscillations emerging from the raster of the population activity. This dual oscillation is also clearly visible from the power spectra (Fig. 8G). The corresponding mean-field only captures the slowest (low-gamma) oscillation (Fig. 9). This reveals that in this case, the mean-field model does not fully capture the complexity of the spiking network. This may be due to the time-scale parameter T which automatically sets a limit to the frequency range that the mean-field model can capture. Further investigations will be necessary to clarify this aspect, but fortunately, these complex oscillation patterns (only seen in Type 2) are rarely seen in these networks. Note that for both types of networks, we generally observed that the magnitude of the oscillation tended to decrease with parameter T (not shown).

Another interesting feature of Type 2 networks is that they may be relevant to the kind of gamma oscillation induced by drugs like Ketamine. Ketamine is known to induce profound changes in brain oscillatory dynamics that appear to be correlated with its antidepressant and sensory dissociative activity (Tian et al. 2023). The electrophysiological profile of sub-anesthetic doses of Ketamine generally includes an increase in gamma oscillation power and a decrease in delta, alpha, and beta oscillation power (Tian et al. 2023). Even though Ketamine is an antagonist of NMDA receptors, several studies have shown that low doses of Ketamine lead to excitation instead of inhibition (Moghaddam et al 1997, Su et al. 2018, Shaw et al 2015). Several hypotheses have been proposed to explain this phenomenon. At low doses, NMDA receptor antagonists preferentially act on NMDA receptors on interneurons (in our study FS cells) instead of those on excitatory neurons, therefore reducing interneuron activity and leading to a disinhibition effect on the overall network activity. It has also been reported that interneurons are more sensitive to NMDAR antagonists than excitatory neurons (Su et al. 2018). A previous computational model (Susin and Destexhe, 2023) has modeled this effect by explicitly including NMDA re-

ceptors in the RS-FS network. In the present model, we did not have NMDA receptors explicitly, but the decrease of the drive onto FS cells mimics a similar effect of reduced excitation of FS cells and a subsequent dis-inhibition of the network. Thus, the gamma oscillations generated in Type 2 networks are probably of a similar type as Ketamine-induced gamma. Indeed it was shown that Ketamine tends to produce low-frequency gamma oscillations (Shaw et al 2015), very similar to our Type 2 model.

Another aspect of gamma-frequency oscillations is that they tend to occur within an asynchronous-irregular (AI) activity state. This was characterized in humans using micro-electrode recordings (Le Van Quyen et al., 2016). The gamma oscillation appears within the AI state and is more present in FS neurons compared to RS neurons, very similar to our model (for example, see Fig. 3 and Fig. 4). This study also found that RS and FS cells are globally in phase, as in our model, but that there was a slight phase advance of FS cells compared to RS cells, which our model did not show. However, previous modeling studies have shown that the exact phase relation between RS and FS cells depends on the parameters (Brunel and Wang, 2003; Susin and Destexhe, 2021), so they do not constitute a good criterion to test the realism of a model.

Future studies should investigate several aspects, in continuation of the present work. The main extension is that this model should be extended to larger scales, by integrating gamma-producing mean-fields in networks of mean-field models (as in Zerlaut et al. 2018). Such an approach can be used to investigate how gamma oscillations organize at large scales in the brain, taking into account long-range connectivity. Since the AdEx mean-field was recently implemented in whole-brain simulations (Goldman et al., 2023), the present mean-field model could form the basis of whole-brain models including gamma-frequency oscillations.

References

[1] Belluscio, Mariano A., Kenji Mizuseki, Robert Schmidt, Richard Kempter, and György Buzsáki. "Cross-frequency phase–phase coupling between theta and gamma oscillations in the hippocampus." Journal of Neuroscience 32, no. 2 (2012): 423-435.

[2] Berke, Joshua D., Murat Okatan, Jennifer Skurski, and Howard B. Eichenbaum. "Oscillatory entrainment of striatal neurons in freely moving rats." Neuron 43, no. 6 (2004): 883-896.

[3] Brunel, Nicolas. "Dynamics of sparsely connected networks of excitatory and inhibitory spiking neurons." Journal of Computational Neuroscience 8 (2000): 183-208.

[4] Brunel Nicolas, and Xiao-Jing Wang. "What determines the frequency of fast network oscillations with irregular neural discharges? I. Synaptic dynamics and excitation-inhibition balance." Journal of Neurophysiology 90, no. 1 (2003): 415-430.

[5] Buzsáki, György, and Xiao-Jing Wang. "Mechanisms of gamma oscillations." Annual review of neuroscience 35 (2012): 203-225.

[6] Chrobak, J., and G. Buzsáki. "Gamma oscillations in the entorhinal cortex of the freely behaving rat." Journal of Neuroscience 18, no. 1 (1998): 388-398.

[7] Di Volo Matteo, Alberto Romagnoni, Cristiano Capone, and Alain Destexhe. "Biologically realistic mean-field models of conductance-based networks of spiking neurons with adaptation." Neural computation 31, no. 4 (2019): 653-680.

[8] Di Volo Matteo, and Torcini Alessandro. "Transition from asynchronous to oscillatory dynamics in balanced spiking networks with instantaneous synapses." Physical review letters 121, no. 12 (2018): 128301.

[9] El Boustani Sami, Destexhe Alain. "A master equation formalism for macroscopic modeling of asynchronous irregular activity states." Neural Computation 21 (2009): 46-100.

[10] Engel, Andreas K., Pascal Fries, and Wolf Singer. "Dynamic predictions: oscillations and synchrony in top–down processing." Nature Reviews Neuroscience 2, no. 10 (2001): 704-716.

[11] Geisler, Caroline, Nicolas Brunel, and Xiao-Jing Wang. "Contributions of intrinsic membrane dynamics to fast network oscillations with irregular neuronal discharges." Journal of Neurophysiology 94, no. 6 (2005): 4344-4361.

[12] Goldman, Jennifer, Lionel Kusch, David Aquilue, Bahar Yalcinkaya, Damien Depannemaecker, Kevin Ancourt, Trang-Anh Nghiem, Viktor Jirsa and Alain Destexhe. "A comprehensive neural simulation of slow-wave sleep and highly responsive wakefulness dynamics." Frontiers in Computational Neuroscience 16 (2023): 1058957.

[13] Gray, Charles M., Peter König, Andreas K. Engel, and Wolf Singer. "Oscillatory responses in cat visual cortex exhibit inter-columnar synchronization which reflects global stimulus properties." Nature 338, no. 6213 (1989): 334-337.

[14] Kayser, Christoph, Robin AA Ince, and Stefano Panzeri. "Analysis of slow (theta) oscillations as a potential temporal reference frame for information coding in sensory cortices." (2012): e1002717.

[15] Le Van Quyen, Michel, Lyle Muller, Bartosz Telenczuk, Sydney Cash, Eric Halgren, Nicho Hatsopoulos, Nima Dehghani and Alain Destexhe. "High-frequency oscillations in human and monkey neocortex during the wake-sleep cycle." Proc. Natl. Acad. Sci. USA 11 (2016): 9363-9368.

[16] Mann, Edward O., Catrin A. Radcliffe, and Ole Paulsen. "Hippocampal gamma-frequency oscillations: from interneurones to pyramidal cells, and back." The Journal of Physiology 562, no. 1 (2005): 55-63.

[17] Moghaddam Bita, Barbara Adams, Anita Verma, and Darron Daly. "Activation of glutamatergic neurotransmission by ketamine: a novel step in the pathway from NMDA receptor blockade to dopaminergic and cognitive disruptions associated with the prefrontal cortex." Journal of Neuroscience 17, no. 8 (1997): 2921-2927.

[18] Popescu, Andrei T., Daniela Popa, and Denis Paré. "Coherent gamma oscillations couple the amygdala and striatum during learning." Nature Neuroscience 12, no. 6 (2009): 801-807.

[19] Shaw, Alexander D., Neeraj Saxena, Laura E. Jackson, Judith E. Hall, Krish D. Singh, and Suresh D. Muthukumaraswamy. "Ketamine amplifies induced gamma frequency oscillations in the human cerebral cortex." European Neuropsychopharmacology 25, no. 8 (2015): 1136-1146.

[20] Sirota, Anton, Sean Montgomery, Shigeyoshi Fujisawa, Yoshikazu Isomura, Michael Zugaro, and György Buzsáki. "Entrainment of neocortical neurons and gamma oscillations by the hippocampal theta rhythm." Neuron 60, no. 4 (2008): 683-697.

[21] Su, Tonghui, Yi Lu, Yang Geng, Wei Lu, and Yelin Chen. "How could N-methyl-D-aspartate receptor antagonists lead to excitation instead of inhibition?." Brain Science Advances 4, no. 2 (2018): 73-98.

[22] Susin, Eduarda, Destexhe Alain. "A network model of the modulation of gamma oscillations by NMDA receptors in cerebral cortex." eNeuro, in press, 2023.

[23] Susin Eduarda, Destexhe Alain. "Integration, coincidence detection and resonance in networks of spiking neurons expressing Gamma oscillations and asynchronous states." PLOS Computational Biology 17, no. 9 (2021): e1009416.

[24] Tian, Fangyun, Laura D. Lewis, David W. Zhou, Gustavo A. Balanza, Angelique C. Paulk, Rina Zelmann, Noam Peled, et al. "Characterizing brain dynamics during ketamine-induced dissociation and subsequent interactions with propofol using human intracranial neurophysiology." Nature communications 14, no. 1 (2023): 1748.

[25] Tort, Adriano BL, Robert Komorowski, Howard Eichenbaum, and Nancy Kopell. "Measuring phase-amplitude coupling between neuronal oscillations of different frequencies." Journal of Neurophysiology 104, no. 2 (2010): 1195-1210.

[26] Wang, Xiao-Jing, and György Buzsáki. "Gamma oscillation by synaptic inhibition in a hippocampal interneuronal network model." Journal of Neuroscience 16, no. 20 (1996): 6402-6413.

[27] Zerlaut, Yann, Sandrine Chemla, Frederic Chavane and Alain Destexhe. "Modeling mesoscopic cortical dynamics using a mean-field model of conductance-based networks of adaptive exponential integrate-and-fire neurons." Journal of Computational Neuroscience 44 (2018): 45-61.

[28] Zerlaut, Yann, and Alain Destexhe. "Enhanced responsiveness and low-level awareness in stochastic network states." Neuron 94, no. 5 (2017): 1002-1009.